Penerbit Akademia Baru

Journal of Advanced Research in Applied Mechanics

Journal homepage: www.akademiabaru.com/aram.html
ISSN: 2289-7895

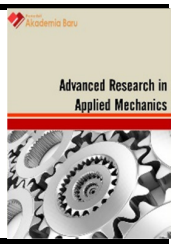

A Bounded Lorentzian Estimation for an Iterative Tomographic Imaging Reconstruction Supported with Lorentzian Regularization

Open Access

Mark Mamdouh[1,*], Osama A. Omer[1,2], Ammar M. Hassan[1,3], Maha Sharkas[1]

[1] Department of Electronics & Communication Engineering, Arab Academy for Science, Technology and Maritime Transport, Aswan, Egypt
[2] Department of Electrical Engineering, Aswan University Aswan 81542, Egypt
[3] Aswan Faculty of Energy Engineering, Aswan University, Aswan, Egypt

ARTICLE INFO

Article history:
Received 5 June 2017
Received in revised form 4 July 2017
Accepted 4 December 2017
Available online 11 March 2018

Keywords:

Computer tomography, L2 norm, Lorentzian norm, reconstruction, regularization

ABSTRACT

Considerable contributions are recently focused on computed tomography (CT) reconstruction methods. Since traditional algorithms based on L2 norm are commonly used, they may degrade the resulting image instead of improving it. In this paper, a bounded-influence M-estimator algorithm based on lorentzian norm has been proposed. Using lorentzian norm for tomographic imaging reconstruction suppresses the outliers due to violations of the observation model while preserving the crispness details. Furthermore, the proposed calculation not only enhances the recreated picture but also upgrades the smoothness constraint where the regularization step is connected with a specific end goal to expel the artifacts from the picture occurring because of associated noise. Experimental results demonstrate that the suggested tomographic imaging calculation has superior robust performance comparing to L2 estimation with L2 regularization model.

1. Introduction

Tomography means imaging a cross-section of an object using either reflected or transmitted data comes from illuminating the object from many different directions [1,2]. In computer tomographic imaging, reproducing an image is really generated from its projections. So, the reconstruction process is mathematically achieved [2].

Tomographic images are basically generated by X-ray devices that produce X-ray penetrating the components of materials to expose hidden particles. There are multiple upgrades in x-ray technology because of advances in electronic components, for more details see [3]. Sharpness, contrast, and the decimation in time have been enhanced by continuous improving X-ray systems

* *Corresponding author.*
E-mail address: mark@aast.edu (Mark Mamdouh)

[4]. Actually, viewing internal organs with precision and safety to the patient became allowable using the X-ray technology. Therefore, diagnostic medicine has improved to be more accurate.

One of common reconstruction algorithms is the filtered back-projection (FBP) algorithm that has a high speed, particularly on dedicated hardware [2][5]. FBP weights all X-rays equally leading to a shortcoming. Since, X-ray tubes produce a polychromatic spectrum, beam-hardening image artifacts arise in the reconstruction.

Many algebraic effective reconstruction calculations have been introduced [2]. Kaczmarz's algorithm [6,7], Randomized Kaczmarz [8], Symmetric Kaczmarz [9], Component Averaging [10], Cimmino [11], and Landweber [12] are common algorithms that are available for training, testing, researching and developing. Numerous such algorithms have been introduced based on L2 statistical norm estimation. These algorithms have a problem where they are usually sensitive to additive noise. So, there is a need for a robust norm which is able to deal with noisy data model in reconstruction calculations.

The proposed recreation algorithm uses the lorentzian norm [13] for killing outliers [14] in the estimated picture. It is handled with an iterative estimation technique in minimizing a cost function. Moreover, lorentzian regularization is used for erasing artifacts from the final estimation and preserving the sharpness edges. The experimental results confirm the effectiveness of the suggested technique and demonstrate its advantages over other reconstruction techniques based on L2 norm.

2. Data Reconstruction Estimation

Tomographic imaging recreation has been essentially produced by received measurements represented as an array of variables. So, reconstruction model is desired to generate a reconstructed picture from projection data.

2.1 Reconstruction Model

A two-dimensional domain is divided into equally spaced intervals in both dimensions creating N cells. For each specified angle θ that is from 0 to 179 in *degrees*, parallel X-rays *p* penetrate the domain. If the picture is square, then the rays are distributed symmetrically around the domain centre. The maximum width of spread rays $w = \sqrt{2N}$; therefore, the number of rays *p* equals to round ($\sqrt{2N}$).

The tomographic image consists of a discrete array of unknown variables x_j, with $j = \{1 \ldots, N\}$, i.e., the unknown factors of attenuation. The system of projections penetrating through the object can easily be modelled by equations of a linear system. Passing through tissue, the intensity of the X-ray beam is weakened according to the attenuation coefficients, x_j. If the image is small, the solution of the corresponding low dimensional linear system of few equations can be obtained, for example, by Gaussian elimination.

Figure 1 introduces a 3x3 pixel image generated by X-ray parallel beams. Nine equations are received with nine unknown values that can be solved exactly, as long as the physical measuring procedure is not afflicted with noise and no linear dependencies occur.

The imaging system can be described as

$$\mathbf{b} = \mathbf{A}\mathbf{x} + \mathbf{n}\,, \tag{1}$$

where **A** is an *M* x *N* weighting matrix, n is the additive noise, and *M* is the whole number of projection rays **b** in all directions. Each weight reflects the relation between the area that is

illuminated by the beam and the pixel entire area. The exact solution of the previous equation (1) is reshaped as a vector **x**. the i^{th} element of **b** is

$$b_i = \sum_{j=1}^{N} a_{ij} x_j, \qquad i = 1, \cdots, length(\theta).p \tag{2}$$

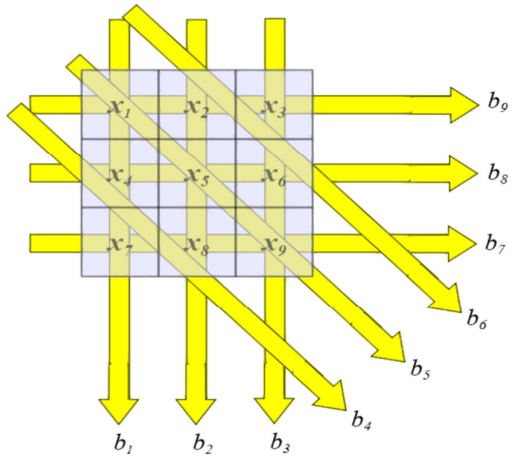

Fig. 1. 3×3 unknown pixels exposed to X-ray parallel beams

Then, we can solve Eq. (1) using iterative algebraic approach. The methods, which use iterative strategies to solve the previous equation, usually start with an initial image, $\mathbf{x}^{(0)}$, a sequence of images, { $\mathbf{x}^{(1)}$, $\mathbf{x}^{(2)}$, . . . }, is calculated iteratively that converges to the desired tomographic picture. In the first step, a forward projection,

$$\mathbf{b}^{(n)} = \mathbf{A}\mathbf{x}^{(n)}, \tag{3}$$

of the n^{th} image approximation $\mathbf{x}^{(n)}$ is determined. The projection, $\mathbf{b}^{(n)}$, determined in the n^{th} forward projection should be compared with the actual measured projection, **b**. The comparison between the determined and the measured projection yields correction terms that are applied to the n^{th} image approximation, $\mathbf{x}^{(n)}$, resulting in the $(n+1)^{th}$ image approximation. This process is iteratively repeated such that with another forward projection, the projection $\mathbf{b}^{(n+1)}$ is determined. Using norm estimators, the solution of Eq. (1) can generally be found by the minimization problem in Eq. (4), where $\rho(\cdot)$ is the error norm.

$$\hat{\mathbf{x}} = \mathrm{ArgMin}_{\mathbf{x}}\{\rho(\mathbf{A}\mathbf{x} - \mathbf{b})\} \tag{4}$$

2.2 L2 norm Estimator

For L2 norm estimators

$$\rho(y) = \|y\|_2^2 \tag{5}$$

Using this estimator with Eq. (4) yields the following minimization problem

$$\hat{\mathbf{x}} = \mathrm{ArgMin}_{\mathbf{x}}\{\|\mathbf{Ax} - \mathbf{b}\|_2^2\} \quad (6)$$

The L2 norm is very sensitive to outliers because the influence function increases gradually linear and without bound [13]. The L2 norm function and its influence function are shown in Figures 2(a) and 2(b), respectively.

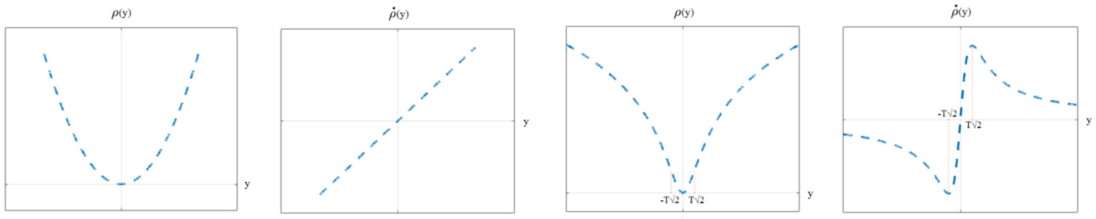

(a) (b) (c) (d)

Fig. 2. Various norm and influence functions (a) L2 norm, (b) L2 norm influence function (c) lorentzian norm, and (d) lorentzian norm influence function

3. Reconstruction with Regulation

The reconstruction process is an ill-posed inversion process because the system matrix A consists of small singular values. Therefore we need to add an additional term for regularization. Also, regularization is used to get rid of artifacts in addition to enhance convergence. Rewriting the cost function of Eq. (4) after adding the regularized term

$$\hat{\mathbf{x}} = \mathrm{ArgMin}_{\mathbf{x}}\{\rho(\mathbf{Ax} - \mathbf{b}) + \lambda \cdot \gamma(\mathbf{x})\} \quad (7)$$

where γ(·) is a regularization function producing the same dimension as the projections column, and λ is a regularization parameter scalar used to control the regularization process.

For L2 norm estimator with L2 Regularization, Eq. (7) has been rewritten as

$$\hat{\mathbf{x}} = \mathrm{ArgMin}_{\mathbf{x}}\{\|\mathbf{Ax} - \mathbf{b}\|_2^2 + \lambda \cdot (\mathbf{\Gamma x})^2\} \quad (8)$$

After using Newton's approach to solve the reconstruction problem in Eq. (8), each-iteration of this algorithm consists of

$$\hat{\mathbf{x}}^{(n+1)} = \hat{\mathbf{x}}^{(n)} - \frac{\dot{\rho} + \lambda \cdot \dot{\gamma}}{\ddot{\rho} + \lambda \cdot \ddot{\gamma}} \quad (9)$$

where $\dot{\rho}$, $\ddot{\rho}$, $\dot{\gamma}$, $\ddot{\gamma}$ are the first and second derivatives of data error norm and regularization function respectively.

4. Proposed Robust Algorithm

4.1 Robust lorentzian norm estimator

For lorentzian norm estimators

$$\rho(y) = \log\left[1 + \frac{1}{2}\left(\frac{y}{T}\right)^2\right] \tag{10}$$

where *T* is a constant that controls outlier threshold. Using this estimator with the minimization problem in Eq. (5), is able to solve the reconstruction problem, where the robust error norm $\rho(\cdot)$ is applied ,element by element, on the error. Lorentzian norm is designed to overcome the problem of outliers by setting a bounding limit at which its influence function reaches zero after exceeding this limit. Lorentzian norm works as; L2 norm for small error, and L1 norm for larger error. Therefore, lorentzian norm was able to have the benefits of L1 and L2 norms while avoiding their drawbacks. Lorentzian norm and its influence function are shown in Figure 2(c) and 2(d), respectively.

The only problem with using a lorentzian norm in the cost function, as a measurements data constraint, is the starting iterations where the data error is very large. This could make the result diverge because the lorentzian is a non-convex function. We can overcome this problem by adopting an initial guess of the data using L2 or any other convex function only for the starting iterations. We can also control the constant *T* of Eq. (10) such that the maximum absolute residual of data measurements is $T\sqrt{2}$ to ensure that the initial estimates contains no outliers and the lorentzian estimator starts with convex approximation.

4.2 Lorentzian norm estimator with lorentzian regularization

Combining lorentzian regularization with lorentzian norm estimator produces

$$\hat{\mathbf{x}} = \mathrm{ArgMin}_{\mathbf{x}}\{\rho(\mathbf{Ax} - \mathbf{b}) + \lambda \cdot \psi(\mathbf{\Gamma x})\}, \tag{11}$$

$$\rho(y) = \log\left[1 + \frac{1}{2}\left(\frac{y}{T}\right)^2\right], \qquad \psi(y) = \log\left[1 + \frac{1}{2}\left(\frac{y}{T_g}\right)^2\right]$$

where *T* and T_g are constants that control outlier thresholds for data constraint and smoothness constraint respectively. After using Newton's approach to solve the reconstruction problem in Eq. (11), each-iteration of this algorithm consists of

$$\hat{\mathbf{x}}^{(n+1)} = \hat{\mathbf{x}}^{(n)} - \frac{\dot{\rho} + \lambda \cdot \dot{\psi}}{\ddot{\rho} + \lambda \cdot \ddot{\psi}} \tag{12}$$

$$\dot{\rho}(y) = \frac{2y}{2T^2 + y^2}, \qquad \ddot{\rho}(y) = \frac{2(2T^2 - y^2)}{(2T^2 + y^2)^2}, \qquad \dot{\psi}(y) = \frac{2y}{2T_g{}^2 + y^2}, \qquad \ddot{\psi}(y) = \frac{2(2T_g{}^2 - y^2)}{(2T_g{}^2 + y^2)^2}$$

5. Results and Discussion

The proposed calculation is applied on a well-known Shepp and Logan "head phantom" image. This image represents a cross section of the human head with X-ray tomography which is commonly used in testing the reconstruction algorithms. The image is described by ten ellipses with different parameters, as shown in Figure 3.

Fig. 3. Shepp and Logan "head phantom" image

To be able to differentiate between the commonly used L2 norm method and our proposed robust algorithm, these methods are applied with the same pattern of random noise. Adding Noise to the received measurement projection values affects the resulting images quality since it degrades the reconstruction process, so we need to add the regularization part to the reconstruction problem as seen in Eq. (7).

Note that, the initial starting guess used in the first iteration was a vector of zeros. Although this starting guess doesn't ensure solution convergence when using our robust algorithm for data constraints, because lorentzian is a non-convex function, but this problem can be solved by controlling the threshold T√2 of the lorentzian function to be equal or greater than any possible data measurement error to ensure the convexity of our model. Furthermore; the proposed algorithm uses updated regularization parameter λ that increases gradually linear to ensure the regularization effect doesn't resist or slow down the reconstruction process in the starting iterations, since the starting guess was a vector of zeros.

After 300 iteration using 768 parallel rays for each 5 degrees of a noisy 256 × 256 parallel beam tomography problem with 5% AWGN level, The results for the traditional L2 norm regularized with L2 smoothness constraint and the robust data constraint regularized with lorentzian smoothness constraint are shown in Figures 4(a) and 4(b) respectively. From these results and from the Peak Signal to Noise Ratio curves shown in Figure 4(c), we find that our robust algorithm is significantly better than L2 for both data and smoothness constraints.

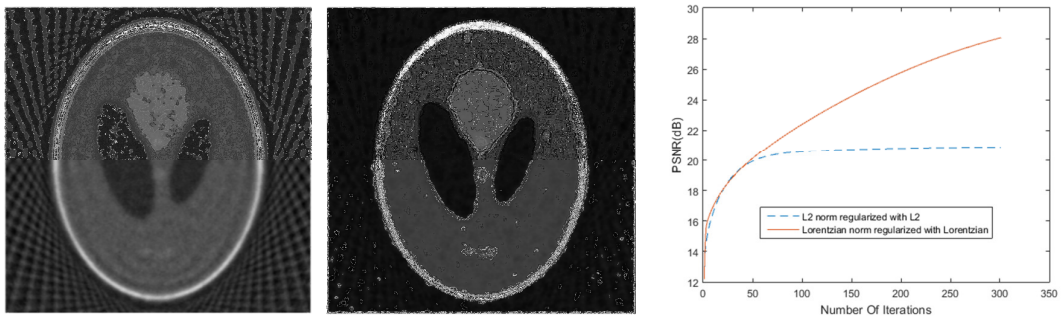

(a) (b) (c)

Fig. 4. Reconstructed images (with PSNR) from noisy measurements (5% AWGN) using; (a) L2 norm for both data and smoothness constraints, and (b) Lorentzian norm for both data and smoothness constraints. (c) PSNR of L2 and lorentzian norms in both data and smoothness constraints

6. Conclusion

The computed tomography reconstruction algorithms that depend on L2 norm estimators have a shortage as reconstruction techniques. So we proposed a robust technique based on lorentzian norm. The proposed algorithm can handle both data and smoothness constraints and produces better results than traditional methods. The experimental results show our proposal superiority over the other techniques especially in the regularization part since it enhances the reconstruction process without modification the outlier differences between neighbour pixels preserving the crispness, high frequency, of the reconstructed image.

References

[1] Buzug, Thorsten M. *Computed tomography: from photon statistics to modern cone-beam CT*. Springer Science & Business Media, 2008.
[2] Avinash C. Kak, and Malcolm Slaney. Principles of computerized tomographic imaging. SIAM, Philadelphia, 2001.
[3] Vaga, Ragnar, and Keith Bryant. "Recent advances in x-ray technology." In *Pan Pacific Microelectronics Symposium (Pan Pacific), 2016*, pp. 1-10. IEEE, 2016.
[4] Duan, Yuping, Dalel Bouslimi, Guanyu Yang, Huazhong Shu, and Gouenou Coatrieux. "Computed Tomography Image Origin Identification Based on Original Sensor Pattern Noise and 3-D Image Reconstruction Algorithm Footprints." *IEEE journal of biomedical and health informatics* 21, no. 4 (2017): 1039-1048.
[5] Zhang, Shu, Youshen Xia, and Changzhong Zou. "Comparison of sparse-view CT image reconstruction algorithms." In *Audio, Language and Image Processing (ICALIP), 2016 International Conference on*, pp. 385-390. IEEE, 2016.
[6] Herman, Gabor T. *Fundamentals of computerized tomography: image reconstruction from projections*. Springer Science & Business Media, 2009.
[7] Kaczmarz, Stefan. "Angenaherte auflosung von systemen linearer gleichungen." *Bull. Int. Acad. Sci. Pologne, A* 35 (1937): 355-357.
[8] Strohmer, Thomas, and Roman Vershynin. "A randomized Kaczmarz algorithm with exponential convergence." *Journal of Fourier Analysis and Applications* 15, no. 2 (2009): 262.
[9] Björck, Åke, and Tommy Elfving. "Accelerated projection methods for computing pseudoinverse solutions of systems of linear equations." *BIT Numerical Mathematics* 19, no. 2 (1979): 145-163.
[10] Censor, Yair, Dan Gordon, and Rachel Gordon. "Component averaging: An efficient iterative parallel algorithm for large and sparse unstructured problems." *Parallel computing* 27, no. 6 (2001): 777-808.
[11] Meyer, C. D. "Matrix Analysis and Applied Linear Algebra Siam, Philadelphia, 2000." *Numerical Algorithms* 26, no. 2 (2001): 198.
[12] Landweber, Louis. "An iteration formula for Fredholm integral equations of the first kind." *American journal of mathematics*73, no. 3 (1951): 615-624.
[13] Patanavijit, Vorapoj, and Somchai Jitapunkul. "A Lorentzian stochastic estimation for a robust iterative multiframe super-resolution reconstruction with Lorentzian-Tikhonov regularization." *EURASIP Journal on Advances in Signal Processing* 2007, no. 2 (2007): 21-21.
[14] Kazantsev, Daniil, Folkert Bleichrodt, Tristan van Leeuwen, Anders Kaestner, Philip J. Withers, Kees Joost Batenburg, and Peter D. Lee. "A Novel Tomographic Reconstruction Method Based on the Robust Student's t Function For Suppressing Data Outliers." *IEEE Transactions on Computational Imaging* 3, no. 4 (2017): 682-693.